Regulation of nuclear–cytoplasmic shuttling and function of Family with sequence similarity 13, member A (Fam13a), by B56-containing PP2As and Akt

Zhigang Jin[a,*], Jin Wei Chung[a,*], Wenyan Mei[a], Stefan Strack[b], Chunyan He[c], Gee W. Lau[d], and Jing Yang[a]

[a]Department of Comparative Biosciences and [d]Department of Pathobiology, College of Veterinary Medicine, University of Illinois at Urbana–Champaign, Urbana, IL 61802; [b]Department of Pharmacology, University of Iowa Carver College of Medicine, Iowa City, IA 52242; [c]Department of Epidemiology, Richard M. Fairbanks School of Public Health, Indiana University, Indianapolis, IN 46202

ABSTRACT **Recent genome-wide association studies reveal that the *FAM13A* gene is associated with human lung function and a variety of lung diseases, including chronic obstructive pulmonary disease, asthma, lung cancer, and pulmonary fibrosis. The biological functions of Fam13a, however, have not been studied. In an effort to identify novel substrates of B56-containing PP2As, we found that B56-containing PP2As and Akt act antagonistically to control reversible phosphorylation of Fam13a on Ser-322. We show that Ser-322 phosphorylation acts as a molecular switch to control the subcellular distribution of Fam13a. Fam13a shuttles between the nucleus and cytoplasm. When Ser-322 is phosphorylated by Akt, the binding between Fam13a and 14-3-3 is enhanced, leading to cytoplasmic sequestration of Fam13a. B56-containing PP2As dephosphorylate phospho–Ser-322 and promote nuclear localization of *Fam13a*. We generated *Fam13a*-knockout mice. *Fam13a*-mutant mice are viable and healthy, indicating that Fam13a is dispensable for embryonic development and physiological functions in adult animals. Intriguingly, Fam13a has the ability to activate the Wnt pathway. Although Wnt signaling remains largely normal in *Fam13a*-knockout lungs, depletion of Fam13a in human lung cancer cells causes an obvious reduction in Wnt signaling activity. Our work provides important clues to elucidating the mechanism by which Fam13a may contribute to human lung diseases.**

Monitoring Editor
Benjamin Margolis
University of Michigan Medical School

Received: Aug 18, 2014
Revised: Jan 12, 2015
Accepted: Jan 14, 2015

INTRODUCTION

Reversible phosphorylation of proteins is a key mechanism that controls the function, localization, and stability of proteins and is important for the vast majority of cellular processes. Phosphorylation occurs most commonly on serine (Ser) and threonine (Thr) residues in proteins. In humans, there are >400 Ser/Thr protein kinases, each recognizing and phosphorylating unique motifs in their substrate proteins (Manning *et al.*, 2002). Of interest, the human genome contains only a dozen genes that encode catalytic subunits of Ser/Thr protein phosphatases, highlighting the importance of these dephosphorylating enzymes.

Protein phosphatase 2A (PP2A) is one of the most abundantly expressed Ser/Thr protein phosphatases, making up to 0.1% of the total cellular protein in most cells. PP2A is a heterotrimer. The holoenzyme is composed of a scaffold (A), a catalytic (C), and a regulatory (B) subunit. The B regulatory subunits are important for the substrate specificity, subcellular localization, and activity of the holoenzyme (Slupe *et al.*, 2011). Recent studies demonstrate that the B56 family of PP2A regulatory subunits (α, β, γ, δ, and ε isoforms) are involved in a wide range of biological processes, including cell

This article was published online ahead of print in MBoC in Press (http://www.molbiolcell.org/cgi/doi/10.1091/mbc.E14-08-1276) on January 21, 2015.

*These authors contributed equally to this work.

Address correspondence to: Jing Yang (yangj@illinois.edu).

Abbreviations used: COPD, chronic obstructive pulmonary disease; Fam13a, Family with sequence similarity 13, member A; GWAS, genome-wide association study; NLS, nuclear localization signal; PP2A, protein phosphatase 2A; SNP, single nucleotide polymorphism.

cycle regulation (Foley *et al.*, 2011; Isoda *et al.*, 2011; Chambon *et al.*, 2013; Kruse *et al.*, 2013; Porter *et al.*, 2013; Xu *et al.*, 2013), apoptosis (Li *et al.*, 2002; Silverstein *et al.*, 2002; Holland *et al.*, 2007; Ruvolo *et al.*, 2008; Jin *et al.*, 2010), embryonic development (Hannus *et al.*, 2002; Yang *et al.*, 2003; Rorick *et al.*, 2007; Jin *et al.*, 2009, 2011; Varadkar *et al.*, 2014), tumorigenesis (Li *et al.*, 2007; Shouse *et al.*, 2008, 2010; Nobumori *et al.*, 2013), and the longevity of worms (Padmanabhan *et al.*, 2009). The crystal structure of B56-containing PP2A has been determined. It has been proposed that B56 uses its concave acidic surface to interact with the basic region on the substrates (Xu *et al.*, 2006; Cho and Xu, 2007). Only a small number of substrates of B56-containing PP2As have been identified. These substrates are involved in a number of major signaling pathways (Virshup and Shenolikar, 2009; Yang and Phiel, 2010). In many cases, how dephosphorylation by B56-containing PP2As alters the function of a protein remains elusive.

B56-containing PP2As play important roles in Wnt signaling. The canonical Wnt pathway is essential for vertebrate axis specification and a variety of developmental processes. It also functions in adult stem cells to regulate adult tissue homeostasis. Dysregulated Wnt signaling causes severe consequences, ranging from defective embryonic development to tumorigenesis in adult animals (Nusse, 2008; MacDonald *et al.*, 2009; van Amerongen and Nusse, 2009; Clevers and Nusse, 2012). Wnt proteins operate the pathway by controlling the stability of β-catenin. In the absence of Wnt, β-catenin is phosphorylated by the β-catenin destruction complex, a cytosolic multiprotein complex consisting of axin, GSK3, APC, etc. Once phosphorylated, β-catenin is rapidly degraded through the ubiquitin/proteasome pathway. Upon binding to their receptors, Wnt proteins initiate an intracellular signaling cascade. Through Dishevelled proteins, Wnts prevents phosphorylation of β-catenin, leading to accumulation of β-catenin in the nucleus, where it activates downstream target genes together with TCF/Lef transcription factors (Clevers and Nusse, 2012). B56s can form a complex with axin and inhibit Wnt signaling by promoting degradation of β-catenin (Seeling *et al.*, 1999; Li *et al.*, 2001). Of interest, knockdown of B56ε, which physically interacts with Dishevelled (Ratcliffe *et al.*, 2000), interferes with Wnt signaling in *Xenopus* embryos (Yang *et al.*, 2003; Jin *et al.*, 2009). It appears that B56-containing PP2As dephosphorylate several components of the Wnt pathway and play a multifaceted role during Wnt signaling.

Results from recent genome-wide association studies (GWASs) indicate that genetic variations in the *FAM13A* gene (Family with sequence similarity 13, member A) are associated with human lung diseases. Using spirometry measurements as markers for lung function, several groups independently discovered that a number of intronic single nucleotide polymorphisms (SNPs) in *FAM13A* are significantly associated with human lung function and chronic obstructive pulmonary disease (COPD; Cho *et al.*, 2010; Hancock *et al.*, 2010; Pillai *et al.*, 2010). Triggered by these finding, *FAM13A* SNPs were tested in other lung diseases. Indeed, an intriguing link between *FAM13A* and asthma severity was identified (Li *et al.*, 2011). In lung cancer, a SNP of *FAM13A*, rs7671167, confers a protective effect, independent of the age, sex, height, lung function, and smoking history of the patients (Young *et al.*, 2011). More recently, *FAM13A* SNPs were found to be associated with pulmonary fibrosis (Fingerlin *et al.*, 2013). In the case of COPD, the *FAM13A* risk SNP rs2609261 is associated with elevated expression of FAM13A in the lung (Kim *et al.*, 2014). These findings suggest that altered expression of Fam13a may contribute to human lung pathological conditions. Nevertheless, the biological function of Fam13a has not been studied.

RESULTS

B56-containing PP2As regulate the subcellular localization of Fam13a

To understand better roles of B56-containing PP2As in controlling intracellular signaling events, we carried out a yeast two-hybrid screen for novel substrates of B56-containing PP2As using B56ε as bait. In addition to known substrates of B56-containing PP2As—for example, axin (Li *et al.*, 2001) and Dzip1 (Jin *et al.*, 2011)—we identified Fam13a. Because SNPs in the *FAM13A* gene are associated with multiple human lung diseases (Cho *et al.*, 2010; Hancock *et al.*, 2010; Pillai *et al.*, 2010; Guo *et al.*, 2011; Li *et al.*, 2011; Young *et al.*, 2011; Fingerlin *et al.*, 2013), we set out to determine whether Fam13a is indeed a substrate of B56-containing PP2As.

We first performed a coimmunoprecipitation in HEK293T cells to verify the interaction between Fam13a and B56ε. We were able to coimmunoprecipitate FAM13A with B56ε (Figure 1A, left). Conversely, B56ε was copurified with Fam13a (Figure 1A, right). As described later, we also performed a yeast two-hybrid screen using Fam13a as bait. Multiple B56 isoforms, including B56α, B56β, B56γ, and B56δ, were retrieved from the screen (unpublished data). Using the yeast two-hybrid system, we directly examined the interaction between Fam13a and all five B56 family members. Indeed, all B56s interacted with Fam13a. According to the growth rate of yeast transformants on selection medium, Fam13a binds B56α, B56β, and B56ε with a higher binding affinity (Table 1). We then generated serial deletion constructs of Fam13a and mapped the B56-binding domain in Fam13a. As shown in Figure 1B, FLAG-B56ε interacted with the full-length and a partially truncated Fam13a (residues 1–609). In contrast, we failed to detect binding between FLAG-B56ε and other truncated forms of Fam13a (1–513, 1–393, 1–341, 1–158). Consistently, Δ513-609, a mutant Fam13a lacking residues 513–609, failed to interact with FLAG-B56ε. We noticed that 515–609 interacted with B56ε very weakly. In contrast, 460–609 strongly interacted with B56ε (Figure 1B). Thus the sequence between residues 460 and 609 of Fam13a, which is conserved across species (Supplemental Figure S1), is sufficient and necessary for B56 binding.

To address whether PP2A regulates Fam13a, we assessed the effect of PP2A inhibition on the subcellular distribution of Fam13a in NIH3T3 cells. Myc-Fam13a was enriched in the nucleus in 85% of control (dimethyl sulfoxide [DMSO]-treated) NIH3T3 cells. Inhibition of PP2A by okadaic acid (OA) treatment altered the subcellular distribution of Fam13a significantly, with 66% of cells exhibiting cytoplasmic Fam13a, ~31% of cells exhibiting homogeneous distribution of Fam13a in nuclear and cytosolic compartments, and only 2% of cells showing nuclear Fam13a (Figure 1C). The effect of OA on subcellular localization of Fam13a was blocked by the nuclear export inhibitor leptomycin B (Supplemental Figure S2), suggesting that OA-induced cytoplasmic localization of Fam13a requires intact nuclear export machinery. Of interest, Fam13a contains a putative nuclear export signal (NES) sequence ($_{672}$-IKAKLRLLEVLI-$_{683}$).

Because Fam13a was originally identified from the screen using B56ε as bait, we determined whether knockdown of B56ε was sufficient to alter the subcellular localization of Fam13a. Of interest, although the level of endogenous B56ε protein was effectively reduced by siB56ε, a small interfering RNA (siRNA) against B56ε (Figure 1D), we failed to detect changes in the subcellular distribution of Fam13a in siB56ε-transfected cells (Figure 1E). This raised the possibility that B56-containing PP2As may function redundantly to control the subcellular localization of Fam13a.

To study redundant functions of B56 subunits, we performed a combinatorial knockdown of all five B56 subunits in the "Aα exchange" cell line. Generated from the PC6-3 subline of PC12 cells

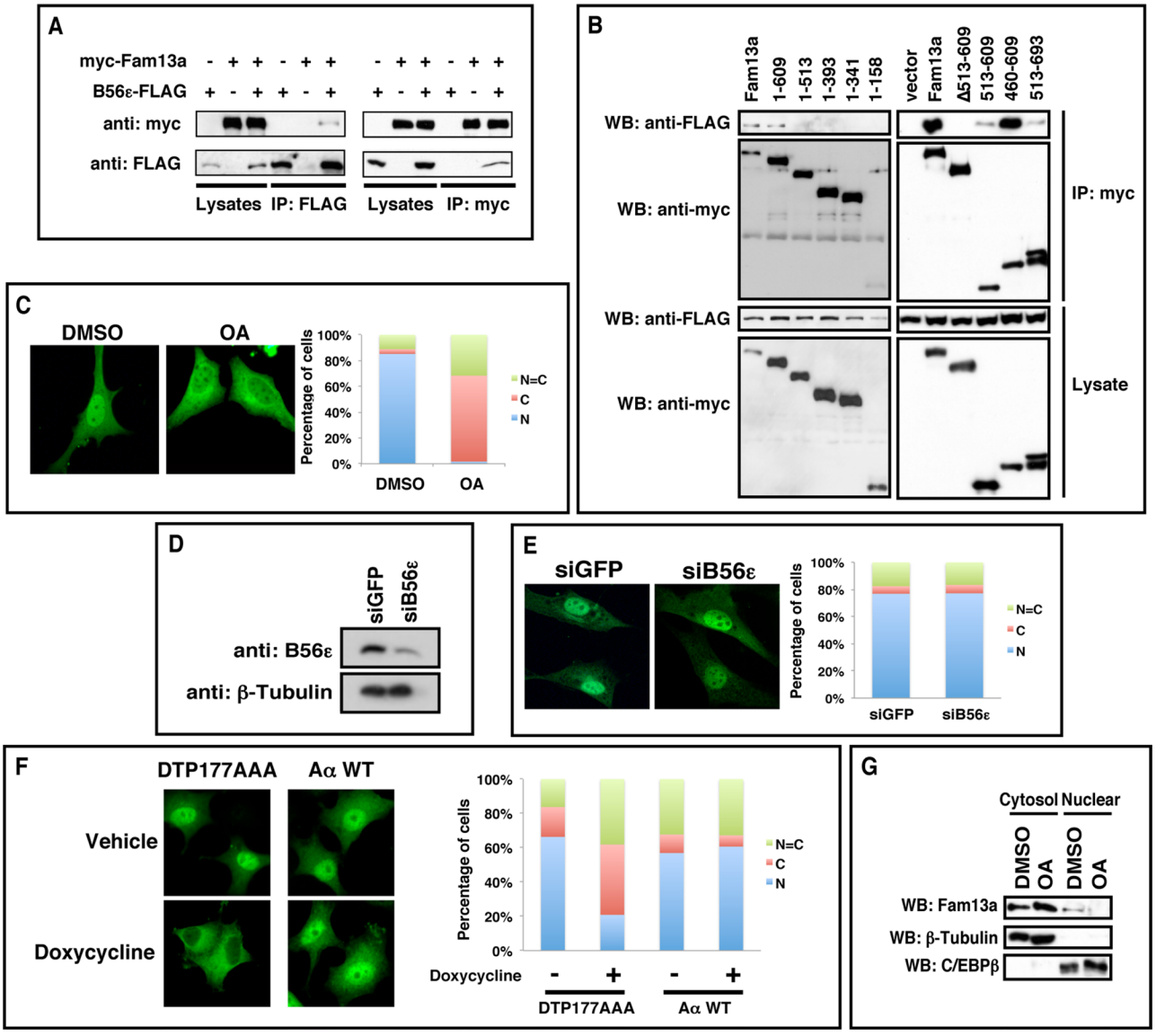

FIGURE 1: B56-containing PP2As regulate nuclear localization of Fam13a. (A) Coimmunoprecipitation (CoIP) showing the interaction between FAM13A and B56ε. B56ε-FLAG and myc-FAM13A were expressed in HEK293T cells alone or in combination. Cells were harvested and subjected to CoIP with an anti-FLAG antibody (left) or an anti-myc antibody (right). (B) Western blot showing that FLAG-B56ε coimmunoprecipitated with full-length Fam13a and 1–609 but not other Fam13a deletion constructs (1–513, 1–393, 1–341, 1–158, and Δ513x609). In addition, FLAG-B56ε strongly interacted with 460–609 but only very weakly with 513–609 and 513–693. (C) Immunofluorescence images showing the nuclear localization of Fam13a in control (DMSO) cells and cytoplasmic localization of Fam13a in OA-treated cells. (D) Western blot showing knockdown of endogenous B56ε by a siRNA against B56ε (siB56ε). (E) Immunofluorescence images showing the nuclear localization of Fam13a in control (siGFP) and B56ε knockdown (siB56ε) cells. (F) Immunofluorescence images showing subcellular localization of wild-type Fam13a in vehicle or doxycycline-treated Aα exchange cells. Wild-type Fam13a was nuclear in vehicle-treated DTP177AAA and AαWT cells. Doxycycline treatment induced cytoplasmic sequestration of Fam13a in DTP177AAA cells but not in AαWT cells. Shown in C, E, and F are representative staining patterns. The percentage of cells displaying nuclear (N), cytoplasmic (C), or even distribution between nucleus and cytoplasm (N = C) are graphed. At least 100 cells from each sample were scored in each experiment. (G) Fractionation of control (DMSO-treated) and OA-treated A549 cells. Endogenous Fam13a protein in nuclear and cytosolic fractions was analyzed by Western blot. β-Tubulin and C/EBPβ served as marker for cytosolic and nuclear fractions, respectively.

(Pittman *et al.*, 1993), Aα exchange cells express both short hairpin RNA (shRNA), which targets the endogenous Aα subunit, and shRNA-resistant mutant Aα from doxycycline-inducible promoters. In Aα exchange cells, doxycycline treatment triggers replacement of the endogenous scaffolding subunit with an Aα mutant (DTP177AAA; Ruediger *et al.*, 1999) that cannot bind B56 subunits. Because free B56 subunits are rapidly degraded through the ubiquitin/proteasome pathway, doxycycline treatment leads to depletion of all B56 isoforms without affecting levels of other PP2A regulatory subunits (Strack *et al.*, 2004). In control cells (Aα WT), doxycycline treatment has no effect on B56 subunit levels because endogenous PP2A A subunit is replaced by a wild-type A subunit,

	pGBKT7-Fam13a
pACT2	–
pACT2-B56α	++
pACT2-B56β	++
pACT2-B56δ	+
pACT2-B56γ	+
pACT2-B56ε	++

Summary of the interaction between B56s and Fam13a in the yeast two-hybrid system. The number of plus signs indicates the relative binding affinity, as judged by the growth rate of yeast transformants.

TABLE 1: Binding between Fam13a and B56 isoforms.

which is capable of binding to B56s (Strack *et al.*, 2004). In Aα DTP177AAA exchange cells, Fam13a was predominantly nuclear in the majority of cells (Figure 1F). Combinatorial knockdown of all B56-containing PP2As by doxycycline treatment induced cytoplasmic sequestration of Fam13a, with only 20% of cells showing nuclear localization of Fam13a. The majority of doxycycline-treated cells exhibited either cytoplasmic (41%) or homogeneous (38%) distribution of Fam13a. Fam13a subcellular distribution remained unaltered in control cells (Aα WT) treated with doxycycline (Figure 1F). This indicates that B56-containing PP2As function redundantly to regulate the nuclear localization of Fam13a.

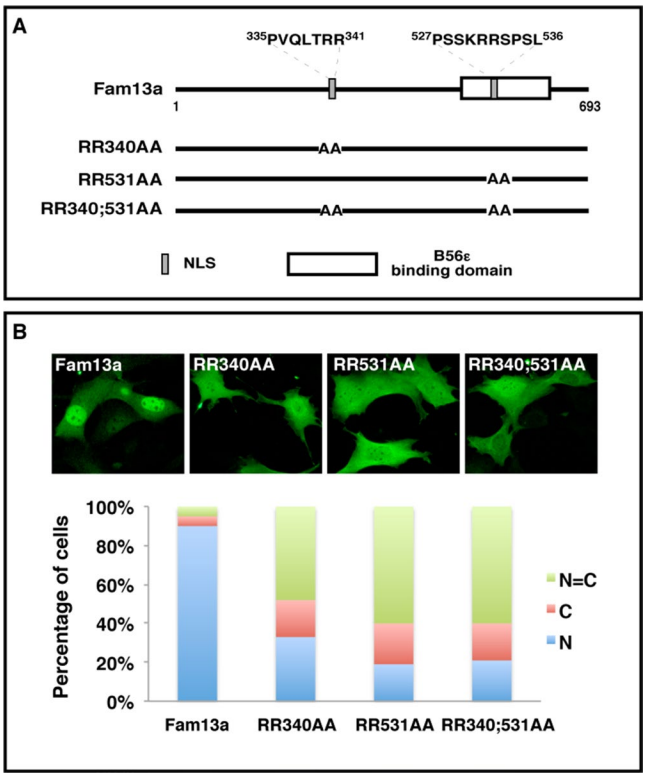

FIGURE 2: Identification of NLSs in Fam13a. (A) Schematic diagram of wild-type Fam13a and NLS mutants (RR340AA, RR531AA, and RR340;531AA). (B) Representative immunofluorescence images showing the nuclear localization of wild-type Fam13a and mislocalization of NLS mutants in NIH3T3 cells. Bar graphs show percentage of cells that exhibit nuclear, cytoplasmic, or homogeneous subcellular distribution. R, arginine; A, alanine.

We further extended our analysis by determining if PP2A regulates the nuclear localization of endogenous Fam13a. Because the anti-Fam13a antibody showed high background in immunostaining, we fractionated A549 human lung cancer cells, in which endogenous Fam13a protein can be detected by Western blot analysis (Supplemental Figure S3). In control A549 cells, Fam13a protein was detected in both cytosolic and nuclear fractions. Inhibition of PP2As by OA treatment increased the amount of cytosolic Fam13a and decreased the amount of nuclear Fam13a (Figure 1G). Taking the results collectively, we conclude that B56-containing PP2As are required for the nuclear localization of Fam13a.

Identification of nuclear localization signals in Fam13a

Using a Web-based nuclear localization signal (NLS) prediction program, we found two arginine/lysine-rich putative NLSs (residues 335–341 and 527–536) in Fam13a protein. To determine whether these putative NLSs sequences are indeed required for the nuclear localization of Fam13a, we mutated these putative NLSs individually (RR340AA and RR531AA) and in combination (RR340;531AA; Figure 2A). The subcellular localization of these constructs was assessed in NIH3T3 cells by immunostaining. As shown earlier, wild-type Fam13a was enriched in the nucleus. In contrast, all three mutants were mislocalized, with the majority of transfected cells (67% of RR340AA, 81% of RR531AA, and 79% of RR340;531AA) exhibiting homogeneous distribution or cytoplasmic accumulation of Fam13a (Figure 2B). These results demonstrate that both NLSs are required for the nuclear localization of Fam13a.

Fam13a interacts with 14-3-3

To gain insights into the function and/or regulation of Fam13a, we carried out a yeast two-hybrid screen for Fam13a-binding proteins using the full-length Fam13a as bait. Apart from several B56 isoforms, >70% of clones identified from this screen carry cDNAs encoding 14-3-3 proteins, including η, ε, ζ, and θ isoforms.

14-3-3 isoforms are highly conserved proteins involved in a wide range of biological processes. In many cases, 14-3-3 proteins sequester their ligands in the cytoplasm. It is also known that binding of 14-3-3 to their ligands requires phosphorylation of a Ser/Thr residue located in the center of the 14-3-3 binding motif (Muslin and Xing, 2000; Aitken, 2006; Freeman and Morrison, 2011; Reinhardt and Yaffe, 2013). We thus hypothesized that inhibition of PP2A enhances phosphorylation of Fam13a, leading to increased binding between Fam13a and 14-3-3. This ultimately results in cytoplasmic sequestration of Fam13a.

To test this hypothesis, we first verified the interaction between Fam13a and 14-3-3s. In a GST pull-down assay, Fam13a was efficiently pulled down by bacterially expressed GST–14-3-3η and GST–14-3-3ε (Figure 3A). When 14-3-3η and Fam13a were coexpressed in HEK293T cells, FLAG–14-3-3η and myc-Fam13a coimmunoprecipitated with each other (Figure 3B). These results suggest that Fam13a and 14-3-3 proteins interact directly. We then mapped the 14-3-3–binding domain using a GST pull-down assay. The full-length and most truncated Fam13a (1–609, 1–513, 1–393, 1–341) were pulled down by GST–14-3-3. By contrast, 1–158 failed to interact with 14-3-3 (Figure 3C), suggesting that 14-3-3 binds to a domain located between residues 158 and 341 in Fam13a. Of interest, a putative 14-3-3 binding motif was found between residues 315 and 329. We generated Δ315–329, a deletion mutant lacking this region. Indeed, truncation of residues 315–329 markedly reduced the binding between 14-3-3 and Fam13a in a GST pull-down assay (Figure 3D). This demonstrates that residues 315–329 are indeed important for binding between Fam13a and 14-3-3. Of note, we

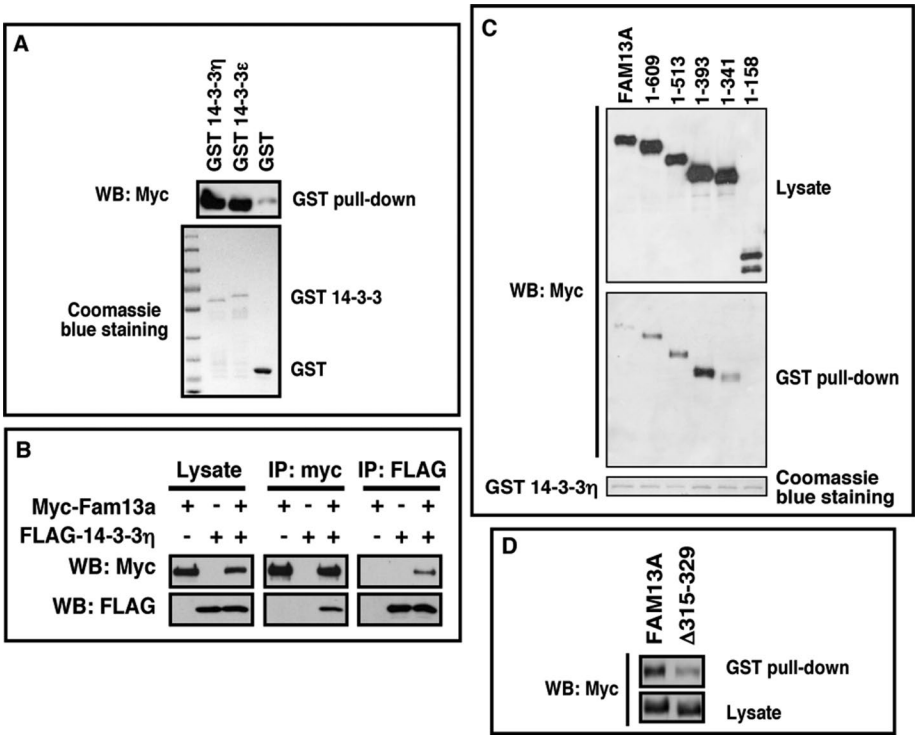

FIGURE 3: Interaction between Fam13a and 14-3-3. (A) GST pull down, showing that Fam13a interacted with bacterially expressed GST–14-3-3η and GST–14-3-3ε but not GST. (B) Western blot, showing coimmunoprecipitation of myc-Fam13a and FLAG–14-3-3η. FLAG–14-3-3η was detected when myc-Fam13a was immunoprecipitated (middle). Conversely, myc-Fam13a was detected when FLAG-14-3-3η was immunoprecipitated (right). (C) GST pull-down assay, showing that GST–14-3-3 interacts with the full-length Fam13a and some Fam13a deletion constructs (1–609, 1–513, 1–393, and 1–341). GST-14-3-3 failed to pull down 1–158. (D) Western blot, showing that truncation of residues 315–329 decreased the binding between GST–14-3-3 and Fam13a.

detected a very weak but reproducible interaction between Δ315–329 and 14-3-3. Our results indicate that Fam13a contains another 14-3-3 binding motif, which is located between residues 404 and 418. Mutation of this 14-3-3 binding motif completely abolished the interaction between Δ315–329 and 14-3-3 (Supplemental Figure S4), indicating that residues 404–418 are responsible for the weak binding between Δ315–329 and 14-3-3.

Next we asked whether residues 315–329, which are important for 14-3-3 binding, are required for cytoplasmic sequestration of Fam13a in response to PP2A inhibition. In control (DMSO-treated) NIH3T3 cells, both Δ315–329 and Fam13a were predominantly nuclear. OA treatment induced cytoplasmic sequestration of Fam13a. In contrast, Δ315–329 remained in the nucleus in the majority of OA-treated cells (61%; Figure 4A). To implicate B56 subunits, we again used Aα DTP177AAA exchange cells. Consistently, depletion of B56-containing PP2As by doxycycline treatment induced cytoplasmic sequestration of wild-type Fam13a but had only minimal effect on Δ315–329 (Figure 4B). These results indicate that the 14-3-3 binding domain (residues 315–329) is required for cytoplasmic sequestration of Fam13a upon inhibition of B56-containing PP2As.

Parallel to the foregoing analyses, we assessed the effects of PP2A inhibition and B56s depletion on the interaction between Fam13a and 14-3-3. We found that OA treatment markedly enhanced the binding between Fam13a and 14-3-3. The effect of OA on this biochemical interaction was reduced significantly by truncation of residues 315–329 (Figure 4C). Consistently, depletion of B56-containing PP2As by doxycycline treatment promoted the interaction between Fam13a and 14-3-3. Truncation of residues 315–329 reduced the effect of B56s knockdown on the binding between Fam13a and 14-3-3 (Figure 4D). These results indicate that inhibition of B56-containing PP2As promotes association of Fam13a with 14-3-3 and cytoplasmic sequestration of Fam13a.

Akt promotes the binding between Fam13a and 14-3-3 and cytoplasmic sequestration of Fam13a

The 14-3-3 proteins preferentially bind to phosphorylated ligands. The 14-3-3 binding motif of Fam13a (residues 315–329) contains a putative Akt recognition motif (RXRXXS/T), raising the possibility that Akt may phosphorylate Fam13a and regulate the subcellular localization of Fam13a by controlling its interaction with 14-3-3 proteins. To test this hypothesis, we asked whether overexpression of myristoylated-Akt (Akt-myr), a constitutively active Akt, could alter the subcellular localization of Fam13a in NIH3T3 cells. We found that when expressed alone, Fam13a was localized in the nucleus in the majority of cells. Coexpression of Akt-myr significantly altered the localization of Fam13a, with ~90% of cells exhibiting either cytoplasmic or homogeneous distribution of Fam13a (Figure 5A).

Next we asked whether Akt is required for cytoplasmic sequestration of Fam13a in response to inhibition of B56-containing PP2As. Consistent with the foregoing observation, Fam13a was primarily nuclear in control (DMSO-treated) cells. OA treatment induced cytoplasmic sequestration of Fam13a, with ~90% of cells showing either cytoplasmic or homogeneous localization (Figure 5B). The majority of cells treated with wortmannin or LY294002, two compounds that inhibit Akt, showed nuclear localization of Fam13a. Strikingly, wortmannin or LY294002 treatment reduced cytoplasmic sequestration of Fam13a induced by OA. Nuclear Fam13a was observed in ~60% of wortmannin/OA- and 85% of LY294002/OA-treated cells (Figure 5B). This demonstrates that Akt-dependent phosphorylation of Fam13a is essential for cytoplasmic sequestration of Fam13a in response to PP2A inhibition.

To assess directly the effect of Akt inhibition on the binding between Fam13a and 14-3-3, we again performed a GST pull-down assay. As expected, OA treatment strongly enhanced the interaction between Fam13a and GST-14-3-3. This OA-induced interaction was significantly reduced by wortmannin treatment (Figure 5C). Collectively our results strongly support the hypothesis that Akt triggers cytoplasmic sequestration of Fam13a by promoting the interaction between Fam13a and 14-3-3 proteins.

Akt and PP2A regulate Ser-322 phosphorylation of Fam13a

Within the 14-3-3 binding motif (residues 315–329), Ser-322 is a putative Akt site. To determine whether Akt and PP2A regulate Fam13a/14-3-3 binding and subcellular localization of Fam13a at least in part by controlling phosphorylation on Ser-322, we blocked Ser-322 phosphorylation by substitution to Ala (S322A). We first

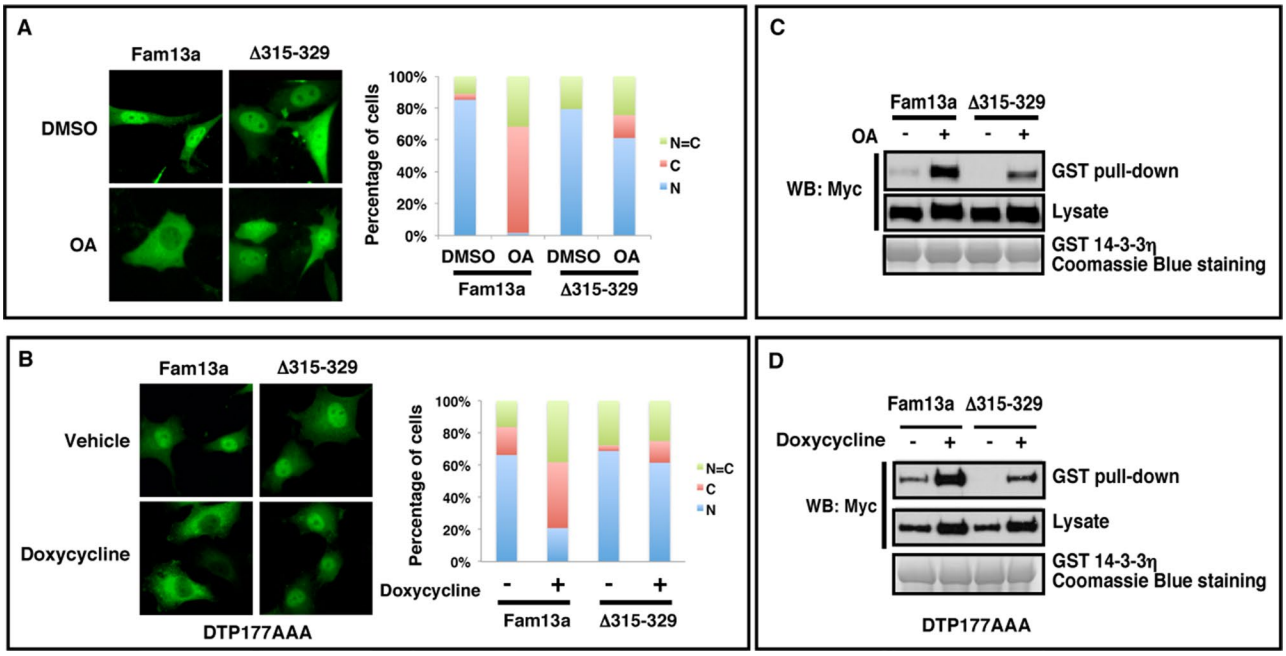

FIGURE 4: The 14-3-3 binding domain is important for cytoplasmic sequestration of Fam13a in response to PP2A inhibition. (A) Representative immunofluorescence images, showing the subcellular distribution of Fam13a and Δ315–329 in control (DMSO) and OA-treated NIH3T3 cells. Fam13a and Δ315–329 were primarily nuclear in control (DMSO) NIH3T3 cells. OA treatment induced cytoplasmic localization of Fam13a. Δ315–329 remained nuclear in the majority of OA-treated cells. (B) Representative immunofluorescence images, showing subcellular distribution of Fam13a and Δ315–329 in control (vehicle-treated) and doxycycline-treated Aα exchange (DTP177AAA) cells. Fam13a and Δ315–329 were nuclear in vehicle-treated cells. After doxycycline treatment, Fam13a was mislocalized. Δ315–329 remained nuclear in the majority of treated cells. Bar graphs in A and B indicate the percentage of cells that exhibit nuclear, cytoplasmic, or homogeneous subcellular distribution. (C) The 14-3-3 binding motif (residues 315–329) is required for the effect of PP2A inhibition on binding between Fam13a and bacterially expressed GST–14-3-3η in a GST pull-down assay. Fam13a- and Δ315–329–expressing cells were treated with DMSO or OA. Cell lysates were used for the GST pull-down assay. Note that OA treatment significantly enhanced interaction between Fam13a and GST–14-3-3. Compared to wild-type Fam13a, Δ315-329 showed much weaker interaction with 14-3-3 after OA treatment. (D) The 14-3-3 binding motif (residues 315–329) is required for the effect of B56s knockdown on binding between Fam13a and GST–14-3-3 in a GST pull-down assay. Fam13a- and Δ315–329–expressing Aα exchange cells were treated with vehicle or doxycycline. Cell lysates were used in a GST pull-down assay. Doxycycline treatment significantly enhanced the interaction between Fam13a and 14-3-3. However, Δ315–329 showed weaker interaction with 14-3-3 compared with wild-type Fam13a after doxycycline treatment.

assessed the subcellular distribution of S322A. Like the wild-type protein, S322A was detected in the nucleus in the majority of cells. When Fam13a- expressing cells were treated with OA, ~70% of cells showed cytoplasmic Fam13a, and the other 30% of cells exhibited homogeneous distribution of Fam13a between the nucleus and cytoplasm. When S322A-expressing cells were treated with OA, only ~15% of cells exhibited predominantly cytosolic localization; the remainder showed either mostly nuclear (~20%) or homogeneous (~65%) localization of the mutant (Figure 6A). We also assessed the binding between S322A and 14-3-3 by GST pull-down assays. We detected weak binding between Fam13a and 14-3-3. By contrast, we failed to detect interaction between S322A and 14-3-3. Inhibition of PP2A by OA treatment caused a dramatic increase in the binding between Fam13a and 14-3-3. When S322A-expressing cells were treated with OA, only a small amount of S322A was pulled down by GST-14-3-3 (Figure 6B). These results suggest that phosphorylation of Fam13a at Ser-322 is important for the binding between Fam13a and 14-3-3 proteins and cytoplasmic sequestration of Fam13a in response to PP2A inhibition.

To assess directly the effects of Akt and PP2A on Ser-322 phosphorylation, we generated an antibody using a peptide that is phosphorylated on Ser-322. This antibody recognizes the wild-type Fam13a but not Δ315–329. It reacted to S322A weakly (Figure 6C). Thus this antibody preferentially recognizes Fam13a that is phosphorylated on Ser-322 (pS322). Using this antibody, we examined the effects of Akt and PP2A on Ser-322 phosphorylation. As shown in Figure 6D, we were able to detect a low level of pSer-322 in DMSO-treated control cells. Inhibition of PP2A by OA caused a robust increase in Ser-322 phosphorylation. Inhibition of Akt by treating cells with wortmannin caused a moderate decrease in Ser-322 phosphorylation. When cells were treated with OA and wortmannin, Ser-322 phosphorylation induced by OA was blunted by wortmannin. We also examined the effects of B56s overexpression on Ser-322 phosphorylation. We found that overexpression of B56β, B56γ, B56δ, and B56ε resulted in a decrease in Ser-322 phosphorylation (Figure 6E), further supporting our conclusion that B56-containing PP2As function redundantly to dephosphorylate Fam13a. Taken together, the foregoing results demonstrate that Ser-322 phosphorylation, which is important for binding between Fam13a and 14-3-3 proteins and cytoplasmic sequestration of Fam13a in response to PP2A inhibition, is indeed controlled by the antagonistic action of Akt and B56-containing PP2As.

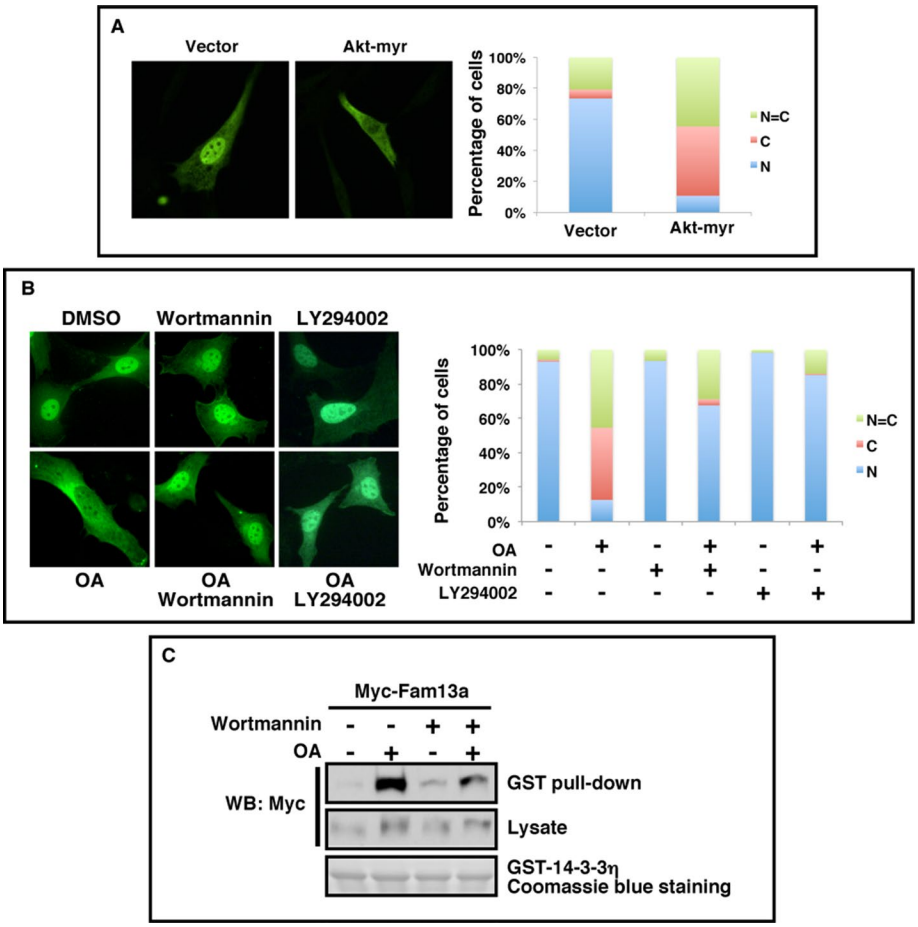

FIGURE 5: Akt promotes cytoplasmic sequestration of Fam13a and binding between Fam13a and 14-3-3. (A) Representative immunofluorescence images, showing the subcellular distribution of Fam13a when cotransfected with an empty vector or Akt-myr in NIH3T3 cells. (B) Representative immunofluorescence images, showing subcellular localization of Fam13a in NIH3T3 cells treated with DMSO (control), OA, wortmannin, LY294002, OA plus wortmannin, or OA plus LY294002. Fam13a localized in the nucleus in control (DMSO) cells. OA-treated cells exhibited cytoplasmic localization of Fam13a. Fam13a remained in the nucleus in wortmannin, LY294002-, OA/wortmannin-, or OA/LY294002-treated cells. Bar graphs in A and B indicate the percentage of cells that exhibit nuclear, cytoplasmic, or homogeneous subcellular distribution. (C) Inhibition of Akt activation by wortmannin reduces OA-induced binding between Fam13a and 14-3-3 in a GST pull-down assay. Fam13a-expressing NIH3T3 cells were treated with DMSO (control), OA, wortmannin, or OA plus wortmannin. Cell lysates were used in a GST pull-down assay. OA treatment strongly enhanced the binding between Fam13a and GST–14-3-3. This effect of OA treatment was reduced by wortmannin treatment. Wortmannin treatment itself had minimal effect on the binding between Fam13a and GST-14-3-3.

Overexpression of Fam13a activates Wnt signaling

To gain insights into the biological function of Fam13a, we carried out gain-of-function studies in *Xenopus* embryos. We found that injection of RNA encoding Fam13a (1 ng) into *Xenopus* embryos induced the formation of partial secondary axes (48%, $n = 52$; Figure 7A). We harvested embryos at the gastrula stage (stage 11) and performed gene expression analysis. We found that overexpression of Fam13a increased the expression of dorsal markers, including *siamois*, *Xnr3*, *chordin*, and *noggin*. The expression of ventral marker *sizzled* was down-regulated. Overexpression of Fam13a had no effect on the expression of *sox17*, a pan-endoderm marker, and *Xbra*, a pan-mesoderm marker (Figure 7B). These results indicate that Fam13a is capable of inducing secondary axis in *Xenopus* embryos.

Wnt signaling plays essential roles during vertebrate axis specification (Heasman, 2006). The observation that overexpression of Fam13a induced axis duplication and increased the expression of *Xnr3* and *siamois*, which are direct targets of Wnt signaling (Lemaire *et al.*, 1995; Smith *et al.*, 1995; Brannon *et al.*, 1997; McKendry *et al.*, 1997), suggests that Fam13a has the ability to activate the Wnt pathway in *Xenopus* embryos. To test this hypothesis, we performed animal cap assays. As expected, overexpression of Fam13a induced the expression of *Xnr3* and *siamois* in animal caps. Fam13a-induced expression of *Xnr3* and *siamois* was not sensitive to Xdd1, a dominant-negative Dishevelled that inhibits the Wnt pathway upstream of the β-catenin destruction complex (Sokol, 1996), but was blocked by axin and GSK3ß, two factors triggering degradation of β-catenin. Overexpression of BMP4, which regulates vertebrate axis specification downstream of the Wnt/*siamois* cascade, did not alter Fam13a-induced expression of *Xnr3* and *siamois* (Figure 7C). Consistently, we found that overexpression of Fam13a increased the expression of β-catenin protein (Figure 7D). It appears that overexpression of Fam13a in *Xenopus* embryos activates the Wnt pathway by stabilizing β-catenin.

Because Fam13a shuttles between the nucleus and cytoplasm, we extended our analysis by determining whether appropriate subcellular localization of Fam13a is important for its function in the Wnt pathway. Thus we compared the activities of Fam13a, Δ315–329, and RR340;531AA in the animal cap assay. The NLS mutant RR340;531AA is homogeneously distributed between the nucleus and cytoplasm (Figure 2). Δ315–329 lacks the 14-3-3 binding domain and is predominantly nuclear even when PP2A is inhibited (Figure 4). As shown in Figure 7E, we found that overexpression of the wild-type Fam13a or Δ315–329 induced the expression of *Xnr3* and *siamois*. In contrast, RR340;531AA showed a very weak activity in this assay. This indicates that Fam13a functions in the nucleus to activate Wnt signaling.

Because Fam13a has been linked to human lung diseases, we determined whether Fam13a could activate Wnt signaling in A549 cells, a widely used human pulmonary epithelial cell model (Giard *et al.*, 1973). As shown in Figure 7F, overexpression of Fam13a increased the expression of β-catenin in A549 cells. Consistently, Fam13a activates TOPFlash, a Wnt-responsive luciferase reporter, and synergizes with β-catenin in the TOPFlash luciferase assay (Figure 7G). Similar to the results obtained from *Xenopus* embryos, the NLS mutant RR340;531AA shows a markedly reduced activity in the TOPFlash assay in A549 cells (Figure 7H). Thus nuclear localization of Fam13a is important for the function of Fam13a in Wnt signaling in human lung cancer cell as well.

Degradation of β-catenin occurs in the cytoplasm (MacDonald *et al.*, 2009; Clevers and Nusse, 2012). The finding that Fam13a functions in the nucleus to activate Wnt signaling suggests that

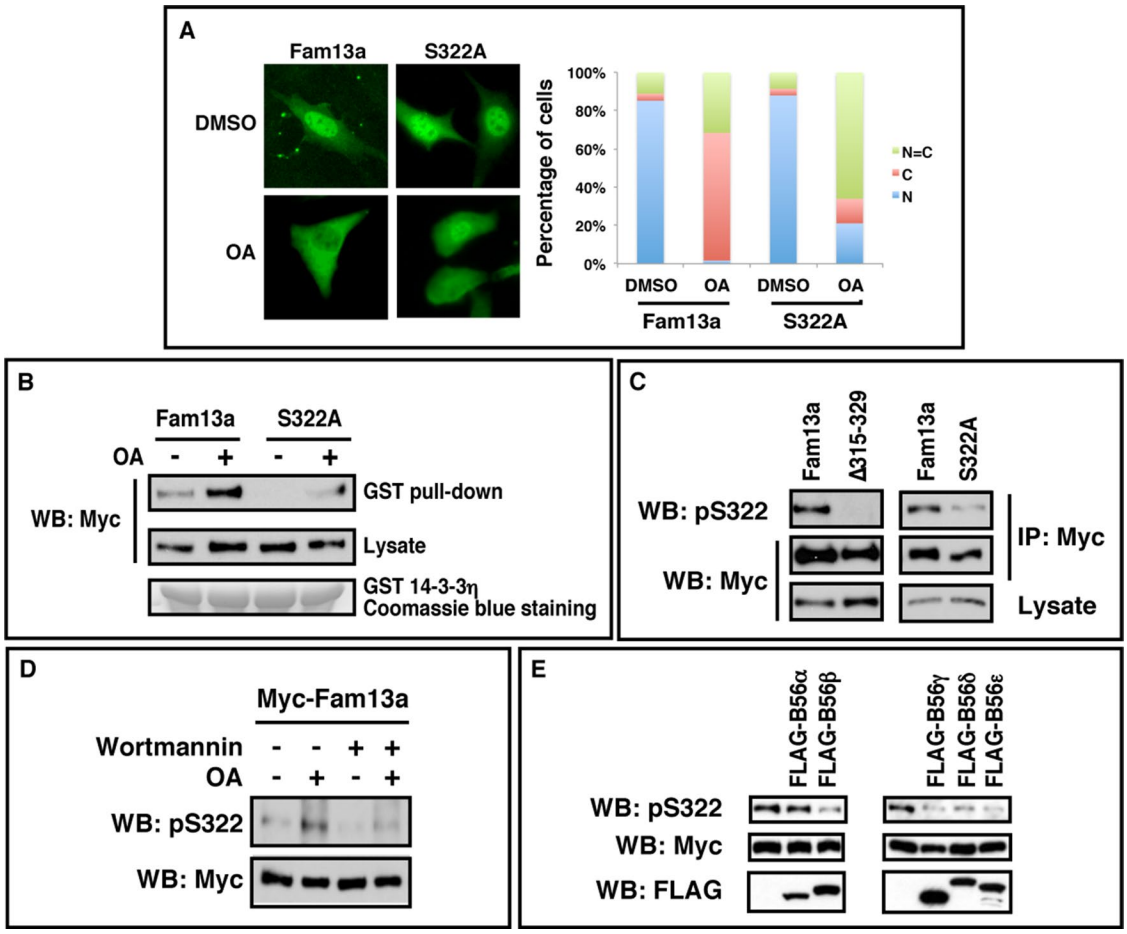

FIGURE 6: Ser-322 is important for subcellular distribution of Fam13a and its interaction with 14-3-3. (A) Representative immunofluorescence images, showing the subcellular distribution of Fam13a and S322A in NIH3T3 cells treated with DMSO (control) or OA. Bar graph indicates the percentage of cells that exhibit nuclear, cytoplasmic, or homogeneous subcellular distribution. (B) A GST pull down, showing that Ser-322 is important for the binding between Fam13a and 14-3-3 and the effect of OA on this interaction. Fam13a- and S322A-expressing NIH3T3 cells were treated with DMSO (control) or OA. Cell lysates were used in a GST pull-down assay. Interaction between Fam13a and 14-3-3 was markedly enhanced in OA-treated cells. In contrast, S322A mutant showed weaker interaction with 14-3-3 in OA-treated cells. (C) Western blot, showing the specificity of the anti-phosphoS322 (pS322) antibody. Note that the anti-pS322 antibody strongly reacted with Fam13a. It did not react with Δ315–329 but recognized S322A weakly. (D) Western blot, showing Ser-322 phosphorylation in NIH3T3 cells treated with DMSO (control), OA, wortmannin, or OA plus wortmannin. pS322 level was increased by OA treatment. The effect of OA on pS322 was reduced by wortmannin treatment. (E) Western blot, showing that overexpression of B56β, B56γ, B56δ, and B56ε decreased Ser-322 phosphorylation. All B56 expression constructs were FLAG tagged.

Fam13a likely stabilizes β-catenin through an indirect mechanism. To gain further insights into the molecular mechanism through which Fam13a regulates ß-catenin, we examined the binding between Fam13a and some components of the β-catenin destruction complex, including GSK3ß and axin. Our results indicate that FLAG-Fam13a forms a complex with myc-axin. In contrast, we failed to detect an interaction between Fam13a and myc-GSK3β (Figure 7I). This indicates that Fam13a is unlikely a component of the β-catenin destruction complex. Strikingly, we found that overexpression of Fam13a decreased the expression of overexpressed HA-axin protein (Figure 7J). It appears that overexpression of Fam13a promotes turnover of axin protein, which leads to stabilization of β-catenin.

Generation of *Fam13a*-knockout mice

The *FAM13A* gene is associated with a number of human lung diseases (Cho *et al.*, 2010; Hancock *et al.*, 2010; Pillai *et al.*, 2010; Guo *et al.*, 2011; Li *et al.*, 2011; Young *et al.*, 2011; Fingerlin *et al.*, 2013). As the first step toward understanding functions of Fam13a in mammals, we analyzed the expression of *FAM13A* in adult mouse tissues by reverse transcription PCR (RT-PCR). Expression of *FAM13A* was detected in all analyzed tissues, except spleen (Figure 8A). We then generated a *FAM13A* floxed allele in which exon5 of the *FAM13A* gene was flanked by *LoxP* sites. After breeding *FAM13A* floxed mice with Sox2-Cre mice, we converted the *FAM13A* floxed allele into a *FAM13A*-knockout allele (Figure 8B). After intercrossing *FAM13A* heterozygous mice, we obtained homozygous *FAM13A* mutants (Figure 8C). These mutants were born at Mendelian ratio and appeared morphologically indistinguishable from their littermates. We extracted RNA from the lungs of wild-type, heterozygous, and homozygous mice and performed RT-PCR. *FAM13A* was detected at their expected sizes in the *FAM13A*$^{+/+}$, *FAM13A*$^{+/-}$, and *FAM13A*$^{-/-}$ lungs (Figure 8D). We sequenced the PCR product and verified that exon 5 was indeed deleted in the *FAM13A*$^{-/-}$ mutant (Figure 8E). Deletion of exon 5 results in a frameshift, leading to truncation of

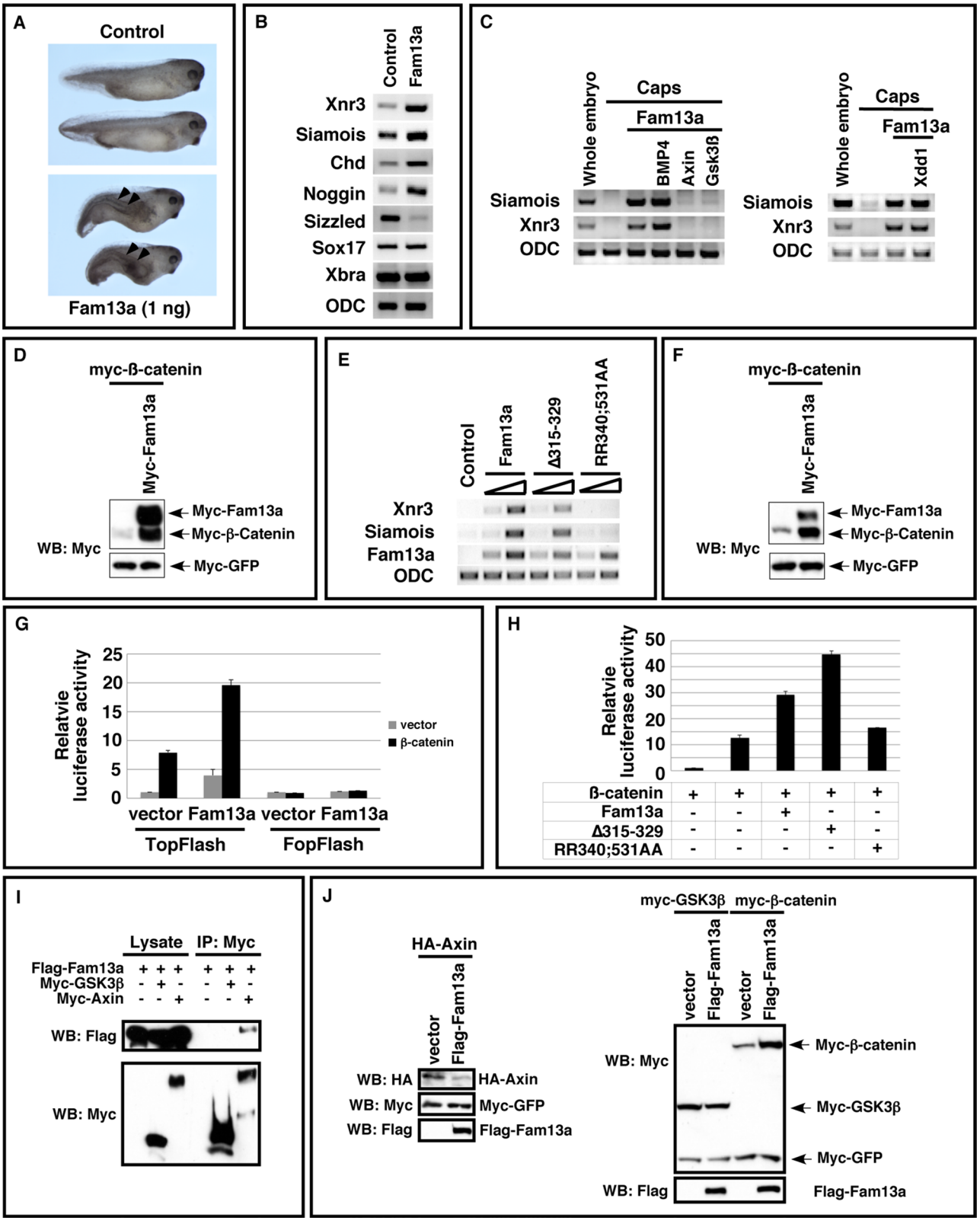

FIGURE 7: Activation of Wnt signaling by Fam13a. (A) Morphology of uninjected and Fam13a RNA (1 ng)–injected *Xenopus* embryos at the tadpole stage. Embryos injected with Fam13a developed partial secondary axes (arrowheads). (B) Expression of *siamois*, *Xnr3*, *chordin*, *noggin*, *sizzled*, *sox17*, and *Xbra* in control and Fam13a-injected embryos. Embryos were harvested at the early gastrula stage. (C) Epistasis analysis showing that the expression of *siamois* and *Xnr3* in Fam13a-overexpressed animal caps was blocked by coexpression of axin or GSK3ß. (D) Western blot showing that overexpression of Fam13a increased the expression of myc–β-catenin in *Xenopus* embryos. At the two-cell stage, embryos were injected with a mixture of myc–β-catenin (100 pg) and myc-GFP (50 pg) RNAs or a mixture of myc–β-catenin, myc-GFP, and myc-Fam13a (1 ng). Embryos were harvested at stage 9. (E) RT-PCR, showing the expression of

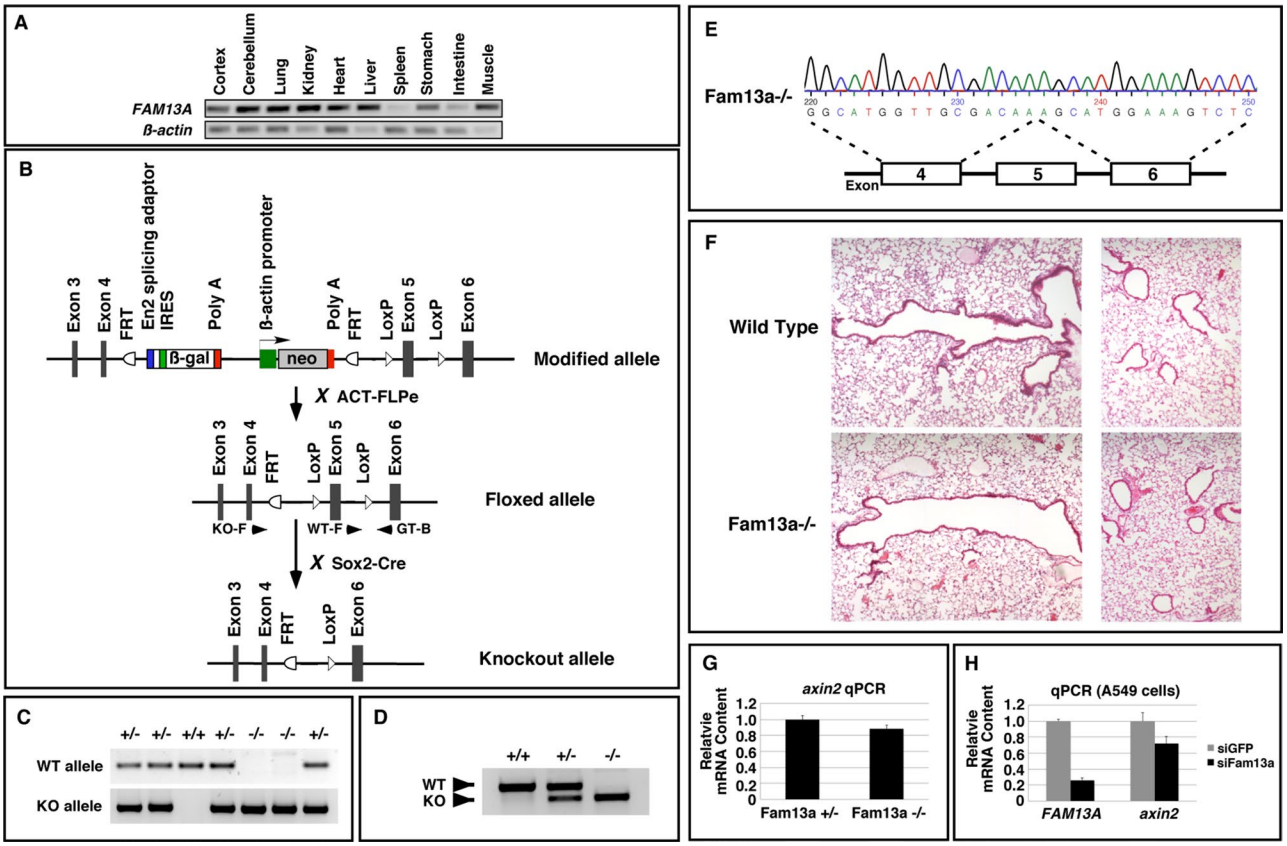

FIGURE 8: Generation and analysis of *Fam13a*-knockout mice. (A) RT-PCR, showing the expression of *FAM13A* in adult mouse tissues. (B) Schematic diagram showing the knockout strategy. Arrowheads indicate primers used for genotyping. KO-F and GT-B were used to detect the knockout allele (KO). WT-F and GT-B were used to detect the wild-type allele (WT). (C) Genotyping PCR showing the genotype of offspring from intercrossing between *Fam13a*$^{+/-}$ mice. (D) RT-PCR, showing the expression of *Fam13a* in wild-type, heterozygous, and knockout animals. (E) Sequence of the PCR product amplified from a *Fam13a*$^{-/-}$-knockout animal, showing deletion of exon 5. (F) Histological analysis of the large airways (left) and alveoli (right) in a wild-type mouse and a *FAM13A*-knockout mouse. (G) Representative real-time RT-PCR result, showing the levels of *axin2* mRNA in control and *Fam13a*$^{-/-}$ lungs. (H) Representative real-time RT-PCR result, showing that knockdown of Fam13a reduced the level of *axin2* mRNA in A549 cells.

Fam13a protein after amino acid residue 97. Given that the *FAM13A* gene is associated with multiple human lung diseases, we examined the lungs from adult *FAM13A*$^{-/-}$ mutants and their wild-type littermates. We failed to detect any morphological difference between the wild-type and *FAM13A*$^{-/-}$-mutant lungs (Figure 8F). Thus Fam13a is dispensable for embryonic and postnatal lung development.

Because overexpression of Fam13a activates the Wnt pathway, we also assessed Wnt signaling activities in the control and *Fam13a*-knockout lungs by examining the transcription of *Axin2*, which is directly regulated by Wnt signaling (Jho *et al.*, 2002). We found that *FAM13A*$^{-/-}$ lung exhibited a very subtle reduction in the level of *axin2* mRNA (Figure 8G). This observation, together with the fact that *FAM13A*$^{-/-}$-mutant mice are morphologically indistinguishable from their littermates, suggests that Fam13a is not essential for Wnt signaling under normal conditions. Of interest, elevated Wnt signaling has been observed in A549 and other human lung cancer cells (You *et al.*, 2004). It has been reported that activation of Wnt signaling accelerates lung tumor growth in transgenic mice carrying an oncogenic Kras (Sidhu *et al.*, 2010). We thus asked whether Fam13a contributes to elevated Wnt signaling in human lung cancer cells. Indeed, we found that knockdown of Fam13a caused a much more obvious reduction in the expression of *axin2* in A549 cells (Figure 8H).

siamois and *Xnr3* in Fam13a-, Δ315–329–, or RR340;531AA-overexpressed animal caps. As a control, the levels of injected Fam13a, Δ315-329, and RR340;531AA RNAs were monitored. (F) Western blot, showing that overexpression of Fam13a increased the expression of myc–β-catenin in A549 cells. (G) Dual-luciferase assays, showing that overexpression of Fam13a activated TOPFlash and enhanced the activity of β-catenin in A549 cells. FOPFlash, which contains mutations in the TCF binding sites, was included as a negative control. Firefly luciferase activity was normalized to the activity of *Renilla* luciferase (TK-RL). (H) Overexpression of Fam13a and Δ315–329, but not RR340;531, enhanced the activity of β-catenin in the TOPFlash luciferase assay in A549 cells. Firefly luciferase activity was normalized to the activity of *Renilla* luciferase. (I) Western blot, showing coimmunoprecipitation of Flag-Fam13a and myc-axin. Of note, we did not detect any interaction between Flag-Fam13a and myc-GSK3β. (J) Western blot showing that overexpression of Fam13a reduced the expression of HA-Axin in A549 cells. The expression level of myc-GSK3ß was not altered by Fam13a overexpression.

It appears that Fam13a is dispensable for Wnt signaling in normal lungs but contributes to the activation of the Wnt pathway in human lung cancer cells.

DISCUSSION

Recent GWASs demonstrate that the *FAM13A* gene is associated with multiple human lung diseases, including COPD, asthma, lung cancer, and pulmonary fibrosis (Cho *et al.*, 2010; Hancock *et al.*, 2010; Pillai *et al.*, 2010; Young *et al.*, 2011; Fingerlin *et al.*, 2013). In the case of COPD, the risk allele is associated with elevated expression of *FAM13A* in the lung (Kim *et al.*, 2014), suggesting that increased expression of Fam13a may have an important contribution to human lung pathological conditions. The biological function of Fam13a has been completely unknown.

Our results provide important clues to elucidate mechanisms through which Fam13a may contribute to human lung diseases. We show that *FAM13A*-knockout mice are viable and healthy. The *FAM13A* mutant lungs are morphologically indistinguishable from wild-type controls. Thus Fam13a is dispensable for embryonic and postnatal lung development. It is also not an essential gene for normal function of the lung in adult animals.

Whereas Fam13a is dispensable under normal conditions, our results reveal that Fam13a is capable of activating Wnt signaling. We show that Fam13a acts in the nucleus to regulate Wnt signaling. Consistent with this result, we failed to detect an interaction between Fam13a and GSK3ß, a key component of the β-catenin destruction complex. These observations argue against a direct role of Fam13a in the β-catenin destruction complex. Of interest, Fam13a interacts with axin and regulates its stability. Axin is a nuclear–cytoplasmic shuttling protein (Cong and Varmus, 2004; Wiechens *et al.*, 2004). It is possible that Fam13a regulates posttranslational of modification(s) of axin in the nucleus, leading to axin turnover. By promoting axin turnover, Fam13a indirectly increases the stability of β-catenin, which ultimately results in Wnt activation. In agreement with this view, we found that overexpression of Fam13a in *Xenopus* embryos activates the expression of Wnt target genes, including *Xnr3* and *siamois*, and triggers the formation of secondary axis. In A549 cells, overexpression of Fam13a induces TOPFlash, a Wnt luciferase reporter. Conversely, depletion of Fam13a in A549 human lung cancer cells or knockout of the mouse *FAM13A* gene leads to a reduction in Wnt signaling activity, judged by decreased transcription of *axin2*, a direct target of Wnt signaling (Jho *et al.*, 2002). Of note, we observed only a subtle reduction in *axin2* transcription in *FAM13A*-knockout lungs, indicating that Fam13a is largely dispensable for Wnt signaling under normal conditions. By contrast, a much more obvious reduction in *axin2* transcription was detected when Fam13a was depleted in A549 cells. This suggests that Fam13a makes a more important contribution to Wnt signaling in human lung cancer cells.

The canonical Wnt pathway plays critical roles in many adult stem cells and is important for tissue homeostasis in a wide rang of lineages (Reya and Clevers, 2005). In adult lungs, most Wnt pathway components are expressed (Winn *et al.*, 2005; Konigshoff *et al.*, 2008). Cigarette smoke, the major cause of many human lung diseases, activates the Wnt pathway in bronchial epithelial cells (Lemjabbar-Alaoui *et al.*, 2006; Liu *et al.*, 2010). Increased Wnt signaling can lead to severe consequences in the lung (Stewart, 2014). In the case of lung cancer, although activation of the Wnt pathway alone is insufficient for triggering lung tumorigenesis, when Wnt signaling is activated in mice carrying an oncogenic Kras, it induces a much more aggressive lung tumor growth (Sidhu *et al.*, 2010). Thus it is possible that due to elevated expression of *FAM13A* (Kim *et al.*, 2014), individuals carrying *FAM13A* risk SNPs may have a more robust Wnt activation in response to cigarette smoke or other harmful inhaled substances, which increases the susceptibility to lung diseases.

It is also worth noting that Fam13a shuttles between the nucleus and cytoplasm. Nuclear localization of Fam13a is important for its function in the Wnt pathway. The subcellular distribution of Fam13a is influenced by the phosphorylation status on Ser-322. Reversible phosphorylation of Ser-322 is controlled by the antagonistic action of Akt and B56-containing PP2As. When Ser-322 is phosphorylated by Akt, the binding between Fam13a and 14-3-3 is enhanced, leading to cytoplasmic sequestration of Fam13a. B56-containing PP2As function redundantly to dephosphorylate Fam13a and promote nuclear localization of Fam13a. Identification of Fam13a as a target of Akt and B56-containing PP2As is of particular interest. It is well known that Akt is involved in a wide range of diseases, including cancers (Franke, 2008). Aberrant Akt signaling has been documented in many human lung diseases, ranging from COPD to lung cancers (David *et al.*, 2004; Bozinovski *et al.*, 2006). In addition, mutations in B56γ (Shouse *et al.*, 2010) and the β isoform of PP2A A subunit (Wang *et al.*, 1998) have been identified from lung cancer patients. It is possible that due to mutations in PP2A or perturbation of Akt under disease conditions, Fam13a becomes mislocalized. This alters the function of Fam13a, which contributes to lung pathological conditions. Further work is needed to test this hypothesis.

In summary, our results demonstrate that Akt and B56-containing PP2As regulate Ser-322 phosphorylation of Fam13a. The phosphorylation status of Ser-322 influences the binding between Fam13a and 14-3-3 and determines the subcellular localization of Fam13a. We provide evidence that nuclear localization of Fam13a is required for its function in the Wnt pathway. Although Fam13a is not essential for Wnt signaling under normal conditions, knockdown of Fam13a significantly reduces the Wnt signaling activity in A549 human lung cancer cells. Our work provides important clues to elucidating the mechanism by which Fam13a may contribute to human lung diseases.

MATERIALS AND METHODS

Yeast two-hybrid screen

An adult mouse brain cDNA library (Clontech, Palo Alto, CA) was screened using full-length *Xenopus* B56ε (pGBKT-B56ε) or mouse Fam13a (pGBKT-Fam13a) as bait, according to standard protocols (*Yeast Protocols Handbook*; Clontech).

Plasmids

The full-length and all deletion constructs of mouse *Fam13a* and mouse *14-3-3*η and *14-3-3ε* expression constructs were generated by standard cloning methods. *B56* expression constructs were described previously (Jin *et al.*, 2009, 2011). Fam13a NLS mutants (RR340AA, RR531AA, and RR340; 531AA), S322A, and Δ315–329;T411A were generated by site-directed mutagenesis. Cloning details will be provided upon request.

Cell culture, transfection, and inhibitor treatments

NIH3T3, HEK293T, PC6-3, and A549 cells were cultured and transfected as described (Strack *et al.*, 2004; Jin *et al.*, 2010). siRNA-mediated knockdown of endogenous B56ε in NIH3T3 or knockdown of endogenous Fam13a in A549 cells was performed using Lipofectamine 2000 transfection reagent (Life Technologies, Gaithersburg, MD). The sequences for the sense and antisense strands of siRNAs are as follows: siGFP, 5′-gcaagcugacccugaaguucuu-3′; 5′-gaacuucaggucagcuugcuu-3′. siB56ε, 5′-ccuagugacagcaaugaauuu-3′; 5′ -auucauugcugucacuagguu-3′. siFam13a, 5′-ggagaacucuuagaaagaauu-3′; 5′-uucuuucuaagaguucuccuu-3′. Knockdown of *B56s* in PC6-3 cells

was carried out as described (Strack *et al.*, 2004; Jin *et al.*, 2011). For PP2A and Akt inhibition studies, NIH3T3 cells were treated with okadaic acid (50 nM, #O7885; Sigma-Aldrich, St. Louis, MO) and/or wortmannin (2 μM, #W1628; Sigma-Aldrich) or LY294002 (#L9908; Sigma-Aldrich) in DMEM supplemented with 0.5% bovine calf serum 1 d after transfection and harvested 15 h after drug administration. For leptomycin B treatment, NIH3T3 cells were exposed to 5 ng/ml leptomycin B (#L2913; Sigma-Aldrich) and/or 50 nM okadaic acid for 15 h before fixation.

Subcellular fractionation

A549 cells were washed twice with ice-cold phosphate-buffered saline (PBS) and scraped into hypotonic buffer containing 10 mM 4-(2-hydroxyethyl)-1-piperazineethanesulfonic acid (HEPES; pH 7.9), 1.5 mM $MgCl_2$, 1 mM EDTA, 10 mM KCl, 0.5 mM dithiothreitol (DTT), and protease inhibitor cocktail. After incubating on ice for 10 min, cells were centrifuged at 13,000 rpm for 5 min, and the supernatant was collected as the cytosol fraction. The pellets were dissolved in a buffer containing 20 mM HEPES (pH 7.9), 1.5 mM $MgCl_2$, 1 mM EDTA, 420 mM NaCl, 25% glycerol, 0.5 mM DTT, and protease inhibitor cocktail. After incubation on ice for 20 min, the sample was centrifuged at 13,000 rpm for 5 min, and the supernatant was collected as the nucleus fraction.

Coimmunoprecipitation, GST pull down, Western blots, and luciferase assay

Coimmunoprecipitation and Western blots were performed as described (Rorick *et al.*, 2007; Jin *et al.*, 2009). For GST pull down, cell lysates were incubated with glutathione beads (#17-0756-01; GE Healthcare, Waukesha, WI) that were immobilized with bacterially expressed GST–14-3-3. Proteins associated with beads were washed extensively, eluted, and analyzed by Western blot. Antibodies used were as follows: anti-Fam13a (1:400; #HPA038109; Sigma-Aldrich), anti-myc (9E10; 1:2000; #5546; Sigma-Aldrich), anti-FLAG (M2, 1:1000; #F1804; Sigma-Aldrich), anti-HA (1:1000; #H9658; Sigma-Aldrich), anti-B56ε (1:400; Jin *et al.*, 2009), anti–β-tubulin (1:1000, #T5293; Sigma-Aldrich) and anti-C/EBPβ (1:400; #sc-150; Santa Cruz Biotechnology, Santa Cruz, CA). Custom anti-pSer-322 antibody was generated by immunizing rabbits with a synthesized peptide (Ac-CFMRRRSS(pS)LG-amide) and subsequent phosphopeptide affinity purification (New England Peptide, Gardner, MA). TOPFlash luciferase reporter assay was performed as described (Veeman *et al.*, 2003; Jin *et al.*, 2011).

RNA extraction, RT-PCR, and PCR purification

RNA purification and RT-PCR were performed as described (Yang *et al.*, 2003). Primers for analyzing *FAM13A* expression in adult mouse tissues were 5′-cctgaggacattaaggatatga-3′ and 5′-tggaggggaaccaatgatg-3′. Primers for *Xnr3*, *siamois*, *noggin*, *sizzled*, *sox17*, *ODC* (Yang *et al.*, 2003; Mei *et al.*, 2013), *chordin*, and *Xbra* have been described (Rorick *et al.*, 2007). Quantitative real-time PCR was performed as described (Jin *et al.*, 2011). Primers were as follows: human *axin2*, 5′-cctgccaccaagacctacat-3′ and 5′-cttcattcaaggtggggaga-3′; human *β-actin*, 5′-agcgggaaatcgtgcgtgac-3′ and 5′-caatggtgatgacctggccgt-3′; mouse *axin2*, 5′-cagcccttgtggttcaagcttc-3′ and 5′-ggtagattcctgatggccgtagt-3′; and mouse *β-actin*, 5′-agagggaaatcgtgcgtgac-3′ and 5′-caatagtgatgacctggccgt-3′.

Xenopus embryos and manipulations

Xenopus embryos were obtained as described (Sive *et al.*, 2000). Microinjection and animal cap assays were performed as described (Sive *et al.*, 2000).

Histological analysis and immunofluorescence

Mouse lungs were inflated, fixed with 4% paraformaldehyde (PFA) overnight at 4°C, washed with PBS, and processed for paraffin embedding according to standard protocols. Sections were cut at 5 μm and stained with hematoxylin and eosin.

For immunostaining, transfected cells were fixed in 4% PFA for 30 min and washed with PBS. Cells were incubated in blocking buffer (1% normal goat serum, 1% bovine serum albumin, 0.1% Triton, PBS) for 30 min at room temperature, followed by incubation with an anti-myc antibody (1:500) overnight at 4°C. Cells were washed with PBS and incubated in Alexa Fluor 488xconjugated anti-mouse antibody (1:500; #A11029; Life Technologies) for 30 min at room temperature. Cells were then washed with PBS and mounted on slides. For the subcellular localization analysis, a minimum of 100 cells were counted for each sample.

Generation and analysis of *FAM13A*-knockout mice

FAM13A-targeted embryonic stem cells (ES cells; KOMP Repository [www.komp.org]) in which exon 5 of the *FAM13A* gene was flanked by *LoxP* sites were used for blastocyst injection (performed by the Transgenic Core Facility at the Research Institute at Nationwide Children's Hospital, Columbus, OH). Male chimeras were bred with wild-type C57BL6 females for germline transmission. Germline-transmitted mice were then bred sequentially with the ACT-FLPe (Jackson Laboratory, Bar Harbor, ME) and Sox2-Cre (Jackson Laboratory) mice to delete the *neo*-cassette and exon 5 of the *FAM13A* gene, respectively. Heterozygous mice carrying the knockout allele were intercrossed to generate homozygous *FAM13A* knockout mice. Primers for genotyping were as follows: wild type forward (WT-F), 5′-gtagtgatgaaggcagagaactg-3′; genotyping backward (GT-B), 5′-ggtaaatgaaagggactgcatg-3′; and knockout allele forward, (KO-F), 5′-acacacacacatatatattccattctag-3′. WT-F and GT-B were used for the wild-type allele. KO-F and GT-B were used for the knockout allele. Primers used for amplification of *FAM13A* mRNA were 5′-tcacaggaagatgaaagacct-3′ and 5′-ctgtcccccaggttctatgc-3′.

ACKNOWLEDGMENTS

The *FAM13A*-knockout mouse strain was created from an ES cell line obtained from the National Center for Research Resources/National Institutes of Health–supported KOMP Repository and generated by the Wellcome Trust Sanger Institute and the Mouse Biology Program (www.mousebiology.org) at the University of California, Davis. This work was supported by National Institutes of Health Grants R01GM093217 to J.Y. and HL090699 and an American Lung Association DeSouza Research Award to G.L., National Institutes of Health Grants R01NS043254 and NS056244 to S.S., an Indiana CTSI Grant, the V-Foundation for Cancer Research Grant, and the Kay Yow Cancer Fund to C.H.

REFERENCES

Aitken A. (2006). 14-3-3 proteins: a historic overview. Semin Cancer Biol 16, 162–172.

Bozinovski S, Vlahos R, Hansen M, Liu K, Anderson GP (2006). Akt in the pathogenesis of COPD. Int J Chronic Obstruct Pulmon Dis 1, 31–38.

Brannon M, Gomperts M, Sumoy L, Moon RT, Kimelman D (1997). A beta-catenin/XTcf-3 complex binds to the siamois promoter to regulate dorsal axis specification in Xenopus. Genes Dev 11, 2359–2370.

Chambon JP, Touati SA, Berneau S, Cladiere D, Hebras C, Groeme R, McDougall A, Wassmann K (2013). The PP2A inhibitor I2PP2A is essential for sister chromatid segregation in oocyte meiosis II. Curr Biol 23, 485–490.

Cho MH, Boutaoui N, Klanderman BJ, Sylvia JS, Ziniti JP, Hersh CP, DeMeo DL, Hunninghake GM, Litonjua AA, Sparrow D, *et al.* (2010). Variants in FAM13A are associated with chronic obstructive pulmonary disease. Nat Genet 42, 200–202.

Cho US, Xu W (2007). Crystal structure of a protein phosphatase 2A heterotrimeric holoenzyme. Nature 445, 53–57.

Clevers H, Nusse R (2012). Wnt/beta-catenin signaling and disease. Cell 149, 1192–1205.

Cong F, Varmus H (2004). Nuclear-cytoplasmic shuttling of Axin regulates subcellular localization of beta-catenin. Proc Natl Acad Sci USA 101, 2882–2887.

David O, Jett J, LeBeau H, Dy G, Hughes J, Friedman M, Brody AR (2004). Phospho-Akt overexpression in non-small cell lung cancer confers significant stage-independent survival disadvantage. Clin Cancer Res 10, 6865–6871.

Fingerlin TE, Murphy E, Zhang W, Peljto AL, Brown KK, Steele MP, Loyd JE, Cosgrove GP, Lynch D, Groshong S, *et al.* (2013). Genome-wide association study identifies multiple susceptibility loci for pulmonary fibrosis. Nat Genet 45, 613–620.

Foley EA, Maldonado M, Kapoor TM (2011). Formation of stable attachments between kinetochores and microtubules depends on the B56-PP2A phosphatase. Nat Cell Biol 13, 1265–1271.

Franke TF (2008). PI3K/Akt: getting it right matters. Oncogene 27, 6473–6488.

Freeman AK, Morrison DK (2011). 14–3-3 Proteins: diverse functions in cell proliferation and cancer progression. Semin Cell Dev Biol 22, 681–687.

Giard DJ, Aaronson SA, Todaro GJ, Arnstein P, Kersey JH, Dosik H, Parks WP (1973). In vitro cultivation of human tumors: establishment of cell lines derived from a series of solid tumors. J Nat Cancer Inst 51, 1417–1423.

Guo Y, Lin H, Gao K, Xu H, Deng X, Zhang Q, Luo Z, Sun S, Deng H (2011). Genetic analysis of IREB2, FAM13A and XRCC5 variants in Chinese Han patients with chronic obstructive pulmonary disease. Biochem Biophys Res Commun 415, 284–287.

Hancock DB, Eijgelsheim M, Wilk JB, Gharib SA, Loehr LR, Marciante KD, Franceschini N, van Durme YM, Chen TH, Barr RG, *et al.* (2010). Meta-analyses of genome-wide association studies identify multiple loci associated with pulmonary function. Nat Genet 42, 45–52.

Hannus M, Feiguin F, Heisenberg CP, Eaton S (2002). Planar cell polarization requires Widerborst, a B′ regulatory subunit of protein phosphatase 2A. Development 129, 3493–3503.

Heasman J (2006). Patterning the early Xenopus embryo. Development 133, 1205–1217.

Holland AJ, Bottger F, Stemmann O, Taylor SS (2007). Protein phosphatase 2A and separase form a complex regulated by separase autocleavage. J Biol Chem 282, 24623–24632.

Isoda M, Sako K, Suzuki K, Nishino K, Nakajo N, Ohe M, Ezaki T, Kanemori Y, Inoue D, Ueno H, Sagata N (2011). Dynamic regulation of Emi2 by Emi2-bound Cdk1/Plk1/CK1 and PP2A-B56 in meiotic arrest of Xenopus eggs. Dev Cell 21, 506–519.

Jho EH, Zhang T, Domon C, Joo CK, Freund JN, Costantini F (2002). Wnt/beta-catenin/Tcf signaling induces the transcription of Axin2, a negative regulator of the signaling pathway. Mol Cell Biol 22, 1172–1183.

Jin Z, Mei W, Strack S, Jia J, Yang J (2011). The antagonistic action of B56-containing protein phosphatase 2As and casein kinase 2 controls the phosphorylation and Gli turnover function of Daz interacting protein 1. J Biol Chem 286, 36171–36179.

Jin Z, Shi J, Saraf A, Mei W, Zhu GZ, Strack S, Yang J (2009). The 48-kDa alternative translation isoform of PP2A:B56epsilon is required for Wnt signaling during midbrain-hindbrain boundary formation. J Biol Chem 284, 7190–7200.

Jin Z, Wallace L, Harper SQ, Yang J (2010). PP2A:B56{epsilon}, a substrate of caspase-3, regulates p53-dependent and p53-independent apoptosis during development. J Biol Chem 285, 34493–34502.

Kim WJ, Lim MN, Hong Y, Silverman EK, Lee JH, Jung BH, Ra SW, Choi HS, Jung YJ, Park YB, *et al.* (2014). Association of lung function genes with chronic obstructive pulmonary disease. Lung 192, 473–480.

Konigshoff M, Balsara N, Pfaff EM, Kramer M, Chrobak I, Seeger W, Eickelberg O (2008). Functional Wnt signaling is increased in idiopathic pulmonary fibrosis. PLoS One 3, e2142.

Kruse T, Zhang G, Larsen MS, Lischetti T, Streicher W, Kragh Nielsen T, Bjorn SP, Nilsson J (2013). Direct binding between BubR1 and B56-PP2A phosphatase complexes regulate mitotic progression. J Cell Sci 126, 1086–1092.

Lemaire P, Garrett N, Gurdon JB (1995). Expression cloning of Siamois, a Xenopus homeobox gene expressed in dorsal-vegetal cells of blastulae and able to induce a complete secondary axis. Cell 81, 85–94.

Lemjabbar-Alaoui H, Dasari V, Sidhu SS, Mengistab A, Finkbeiner W, Gallup M, Basbaum C (2006). Wnt and Hedgehog are critical mediators of cigarette smoke-induced lung cancer. PLoS One 1, e93.

Li HH, Cai X, Shouse GP, Piluso LG, Liu X (2007). A specific PP2A regulatory subunit, B56gamma, mediates DNA damage-induced dephosphorylation of p53 at Thr55. EMBO J 26, 402–411.

Li X, Howard TD, Moore WC, Ampleford EJ, Li H, Busse WW, Calhoun WJ, Castro M, Chung KF, Erzurum SC, *et al.* (2011). Importance of hedgehog interacting protein and other lung function genes in asthma. J Allergy Clin Immunol 127, 1457–1465.

Li X, Scuderi A, Letsou A, Virshup DM (2002). B56-associated protein phosphatase 2A is required for survival and protects from apoptosis in Drosophila melanogaster. Mol Cell Biol 22, 3674–3684.

Li X, Yost HJ, Virshup DM, Seeling JM (2001). Protein phosphatase 2A and its B56 regulatory subunit inhibit Wnt signaling in Xenopus. EMBO J 20, 4122–4131.

Liu F, Killian JK, Yang M, Walker RL, Hong JA, Zhang M, Davis S, Zhang Y, Hussain M, Xi S, *et al.* (2010). Epigenomic alterations and gene expression profiles in respiratory epithelia exposed to cigarette smoke condensate. Oncogene 29, 3650–3664.

MacDonald BT, Tamai K, He X (2009). Wnt/beta-catenin signaling: components, mechanisms, and diseases. Dev Cell 17, 9–26.

Manning G, Whyte DB, Martinez R, Hunter T, Sudarsanam S (2002). The protein kinase complement of the human genome. Science 298, 1912–1934.

McKendry R, Hsu SC, Harland RM, Grosschedl R (1997). LEF-1/TCF proteins mediate wnt-inducible transcription from the Xenopus nodal-related 3 promoter. Dev Biol 192, 420–431.

Mei W, Jin Z, Lai F, Schwend T, Houston DW, King ML, Yang J (2013). Maternal Dead-End1 is required for vegetal cortical microtubule assembly during Xenopus axis specification. Development 140, 2334–2344.

Muslin AJ, Xing H (2000). 14–3-3 proteins: regulation of subcellular localization by molecular interference. Cell Signal 12, 703–709.

Nobumori Y, Shouse GP, Wu Y, Lee KJ, Shen B, Liu X (2013). B56gamma tumor-associated mutations provide new mechanisms for B56gamma-PP2A tumor suppressor activity. Mol Cancer Res 11, 995–1003.

Nusse R (2008). Wnt signaling and stem cell control. Cell Res 18, 523–527.

Padmanabhan S, Mukhopadhyay A, Narasimhan SD, Tesz G, Czech MP, Tissenbaum HA (2009). A PP2A regulatory subunit regulates C. elegans insulin/IGF-1 signaling by modulating AKT-1 phosphorylation. Cell 136, 939–951.

Pillai SG, Kong X, Edwards LD, Cho MH, Anderson WH, Coxson HO, Lomas DA, Silverman EK (2010). Loci identified by genome-wide association studies influence different disease-related phenotypes in chronic obstructive pulmonary disease. Am J Respir Crit Care Med 182, 1498–1505.

Pittman RN, Wang S, DiBenedetto AJ, Mills JC (1993). A system for characterizing cellular and molecular events in programmed neuronal cell death. J Neurosci 13, 3669–3680.

Porter IM, Schleicher K, Porter M, Swedlow JR (2013). Bod1 regulates protein phosphatase 2A at mitotic kinetochores. Nat Commun 4, 2677.

Ratcliffe MJ, Itoh K, Sokol SY (2000). A positive role for the PP2A catalytic subunit in Wnt signal transduction. J Biol Chem 275, 35680–35683.

Reinhardt HC, Yaffe MB (2013). Phospho-Ser/Thr-binding domains: navigating the cell cycle and DNA damage response. Nat Rev Mol Cell Biol 14, 563–580.

Reya T, Clevers H (2005). Wnt signalling in stem cells and cancer. Nature 434, 843–850.

Rorick AM, Mei W, Liette NL, Phiel C, El-Hodiri HM, Yang J (2007). PP2A:B56epsilon is required for eye induction and eye field separation. Dev Biol 302, 477–493.

Ruediger R, Fields K, Walter G (1999). Binding specificity of protein phosphatase 2A core enzyme for regulatory B subunits and T antigens. J Virol 73, 839–842.

Ruvolo VR, Kurinna SM, Karanjeet KB, Schuster TF, Martelli AM, McCubrey JA, Ruvolo PP (2008). PKR regulates B56(alpha)-mediated BCL2 phosphatase activity in acute lymphoblastic leukemia-derived REH cells. J Biol Chem 283, 35474–35485.

Seeling JM, Miller JR, Gil R, Moon RT, White R, Virshup DM (1999). Regulation of beta-catenin signaling by the B56 subunit of protein phosphatase 2A. Science 283, 2089–2091.

Shouse GP, Cai X, Liu X (2008). Serine 15 phosphorylation of p53 directs its interaction with B56gamma and the tumor suppressor activity of B56gamma-specific protein phosphatase 2A. Mol Cell Biol 28, 448–456.

Shouse GP, Nobumori Y, Liu X (2010). A B56gamma mutation in lung cancer disrupts the p53-dependent tumor-suppressor function of protein phosphatase 2A. Oncogene 29, 3933–3941.
Sidhu SS, Nawroth R, Retz M, Lemjabbar-Alaoui H, Dasari V, Basbaum C (2010). EMMPRIN regulates the canonical Wnt/beta-catenin signaling pathway, a potential role in accelerating lung tumorigenesis. Oncogene 29, 4145–4156.
Silverstein AM, Barrow CA, Davis AJ, Mumby MC (2002). Actions of PP2A on the MAP kinase pathway and apoptosis are mediated by distinct regulatory subunits. Proc Natl Acad Sci USA 99, 4221–4226.
Sive H, Grainger R, Harland R (2000). Early Development of Xenopus laevis. A Laboratory Manual, Cold Spring Harbor, NY: Cold Spring Harbor Press.
Slupe AM, Merrill RA, Strack S (2011). Determinants for substrate specificity of protein phosphatase 2A. Enzyme Res 2011, 398751.
Smith WC, McKendry R, Ribisi S Jr, Harland RM (1995). A nodal-related gene defines a physical and functional domain within the Spemann organizer. Cell 82, 37–46.
Sokol SY (1996). Analysis of Dishevelled signalling pathways during Xenopus development. Curr Biol 6, 1456–1467.
Stewart DJ (2014). Wnt signaling pathway in non-small cell lung cancer. J Nat Cancer Inst 106, djt356.
Strack S, Cribbs JT, Gomez L (2004). Critical role for protein phosphatase 2A heterotrimers in mammalian cell survival. J Biol Chem 279, 47732–47739.
van Amerongen R, Nusse R (2009). Towards an integrated view of Wnt signaling in development. Development 136, 3205–3214.
Varadkar P, Despres D, Kraman M, Lozier J, Phadke A, Nagaraju K, McCright B (2014). The protein phosphatase 2A B56gamma regulatory subunit is required for heart development. Dev Dyn 243, 778–790.
Veeman MT, Slusarski DC, Kaykas A, Louie SH, Moon RT (2003). Zebrafish prickle, a modulator of noncanonical Wnt/Fz signaling, regulates gastrulation movements. Curr Biol 13, 680–685.
Virshup DM, Shenolikar S (2009). From promiscuity to precision: protein phosphatases get a makeover. Mol Cell 33, 537–545.
Wang SS, Esplin ED, Li JL, Huang L, Gazdar A, Minna J, Evans GA (1998). Alterations of the PPP2R1B gene in human lung and colon cancer. Science 282, 284–287.
Wiechens N, Heinle K, Englmeier L, Schohl A, Fagotto F (2004). Nucleo-cytoplasmic shuttling of Axin, a negative regulator of the Wnt-beta-catenin pathway. J Biol Chem 279, 5263–5267.
Winn RA, Marek L, Han SY, Rodriguez K, Rodriguez N, Hammond M, Van Scoyk M, Acosta H, Mirus J, Barry N, *et al.* (2005). Restoration of Wnt-7a expression reverses non-small cell lung cancer cellular transformation through frizzled-9-mediated growth inhibition and promotion of cell differentiation. J Biol Chem 280, 19625–19634.
Xu P, Raetz EA, Kitagawa M, Virshup DM, Lee SH (2013). BUBR1 recruits PP2A via the B56 family of targeting subunits to promote chromosome congression. Biol Open 2, 479–486.
Xu Y, Xing Y, Chen Y, Chao Y, Lin Z, Fan E, Yu JW, Strack S, Jeffrey PD, Shi Y (2006). Structure of the protein phosphatase 2A holoenzyme. Cell 127, 1239–1251.
Yang J, Phiel C (2010). Functions of B56-containing PP2As in major developmental and cancer signaling pathways. Life Sci 87, 659–666.
Yang J, Wu J, Tan C, Klein PS (2003). PP2A:B56epsilon is required for Wnt/beta-catenin signaling during embryonic development. Development 130, 5569–5578.
You L, He B, Xu Z, Uematsu K, Mazieres J, Mikami I, Reguart N, Moody TW, Kitajewski J, McCormick F, Jablons DM (2004). Inhibition of Wnt-2-mediated signaling induces programmed cell death in non-small-cell lung cancer cells. Oncogene 23, 6170–6174.
Young RP, Hopkins RJ, Hay BA, Whittington CF, Epton MJ, Gamble DG (2011). FAM13A locus in COPD is independently associated with lung cancer—evidence of a molecular genetic link between COPD and lung cancer. Appl Clin Genet 4, 1–10.